Indices of Congested Areas and Contributions of Customers to Congestions in Radial Distribution Networks

Jinping Zhao, Ali Arefi, Alberto Borghetti, and Gerard Ledwich

Abstract—Congestions are becoming a significant issue with an increasing number of occurrences in distribution networks due to the growing penetration of distributed generation and the expected development of electric mobility. Fair congestion management (CM) policies and prices require proper indices of congested areas and contributions of customer to congestions. This paper presents spatial and temporal indices for rapidly recognizing the seriousness of congestions from the perspectives of both magnitude violation and duration to prioritize the affected areas where CM procedures should be primarily activated. Besides, indices are presented which describe the contributions of customers to the congestions. Simulation tests on IEEE 123-bus and Australian 23-bus low-voltage distribution test feeders illustrate the calculation and capabilities of the proposed indices in balanced and unbalanced systems.

Index Terms—Congestion management, spatial index, temporal index, distribution network, contribution of customer.

I. INTRODUCTION

THE operation and control of distribution networks are undergoing significant changes due to the large number of active customers and new types of loads such as air conditioners, heat pumps, and electric vehicles (EVs) [1], [2]. With the growing penetration of generation from renewable energy [3], e. g., photovoltaic (PV), and increasing load, there is the need for the development of improved congestion management (CM) procedures in distribution networks [4].

Traditionally, the congestion happens when sufficient energy cannot be transmitted to customers due to aged equipment, ineffective network planning, faults, and the low accuracy of the load forecasts [5]. In distribution networks, congestions often occur due to the rapid increase in the penetration of distributed generation (DG), sudden rise of load growth, the installation of EV charging stations without adequate planning [6], [7], and the electrification of heating systems. Massive power injection from DGs will give rise to the congestion with over-voltage issues, and specific control approaches are needed to relieve voltage violations [8], [9]. The intermittency of DG output power and the randomness of the EV charging result in the durations and frequencies of the congestion varying significantly in different periods. Flexibilities from active customers via a dedicated market [10] or active distribution management systems [11] are considered as essential components of CM procedures in distribution networks. In this context, improved monitoring of congestions is needed. Short-term, e. g., 24 hours, and long-term, e. g., a year, congestion estimations can provide useful information for adopting CM strategies in flexibility regulation, system planning, and investments.

The duration, extension, and levels of expected congestions need to be determined to assess the adequacy and performances of a CM procedure. The direction of power flow suggests the congestion scenario. If the power flows from the substation to load, the power output of DG can help the system to relieve the congestion in some areas, while if the direction is opposite, the output from DG is the main reason for the congestion. In some cases, the intervention of CM procedures is not required when there is a slight congestion for a short time due to fluctuating load and growing uncertainties. Appropriate indices are needed to promptly recognize the seriousness of congestions. Moreover, they can be a reference for the design of fair CM policies [12].

Compared with the studies regarding CM in transmission networks, the research on prediction and management of congestions in distribution systems is still limited. So far, overloading, and locational marginal prices (LMPs) are utilized to identify the seriousness of congestions for the wholesale power markets. In transmission networks, higher electricity prices appear in case of overload of transmission lines [13]. The values of LMP can indicate the congestion level. The CM method proposed in [14] prevents line overloading by applying a cost/curvature constrained power flow optimization.

Similarly, load reduction and costs are the primary components to minimize the objective function considered in [15]. Power flow constraint violation and generation capacity lim-

J. Zhao (corresponding author) and A. Arefi are with the College of Science, Health, Engineering, and Education, Murdoch University, WA, 6150, Australia (e-mail: jinping.zhao@murdoch.edu.au; ali.arefi@murdoch.edu.au).

A. Borghetti is with the Department of Electrical, Electronic, and Information Engineering, University of Bologna, Bologna, 40126, Italy (e-mail: alberto.borghetti@unibo.it).

G. Ledwich is with the School of Electrical Engineering and Robotics, Queensland University of Technology, Brisbane, QLD 4000, Australia (e-mail: g.ledwich@qut.edu.au).

its are the two indicators considered in [16], [17], whilst voltage and transient stability margins are included in [18]. For the CM based on bilateral contracts among participants combined with probabilistic optimal power flow (POPF) presented in [16], congestion distribution factors (CDFs) are proposed to customers into different clusters by their impacts on constrained transmission lines. The congestion is also defined by explicitly considering the presence of renewable generation in [19].

In distribution networks, overloading and voltage violation are the two main concerns [20]-[22]. The percentage of time that power flow exceeds the constraint of a line is defined as the risk of congestion in [23].

The estimation of the congestion severity has some peculiarities with respect to probabilistic load flow analysis. While probabilistic load flow is concerned with estimated system states and short- or long-term planning [24], the assessment of congestion severity focuses on the level of thermal limit violations and voltage violations that can cause equipment issues, unsatisfied load demand, and DG curtailment.

The improved implementation of all the flexibilities is required for fair and efficient CM procedures and markets, intending to maximize the active participation of all the users. DG and demand response (DR) are expected to help in the CM of transmission networks, as described in [17], [18], [25]-[27]. Dynamic tariff subsidy and asymmetric block offer to the electricity market are proposed in [21], [22] for the deployment of DR in CM. The role of storage units is also promising, as analyzed in [28], [29]. For the implementation of these schemes, the contributions of customers to congestions and their solution need to be calculated. Moreover, improved market policy and regulation schemes can be achieved by considering long-term contribution indices.

The shortcomings in the literature mentioned above are as follows.

1) Although overloading increased LMPs, and voltage violations are indicators for the occurrence of congestions in distribution systems, an additional analysis is needed for the definition of indices that can be utilized to estimate the severity of congestions both in the short term and long term.

2) Long-term congestion estimation, network planning, and investment decisions require improved indices to better capture the intermittent characteristic, frequency, and duration of congestions.

3) There is still a lack of aggregate indices, combining both temporal and spatial aspects, able to recognize and prioritize the congested areas.

This paper aims at presenting indices that better reveal the severity of congestion and monitor the specific contributions to congestion by the customers connected to each bus in the long-term horizon. A clear indication of congestion severity and contributions of customer to congested areas will help utility operators to recognize problems and activate a fair CM procedure promptly.

The long-term estimation of congested areas and contributions of customers can be derived from the clustering of power flow conditions. The analysis considers both the daily violations of the branch thermal limits and the voltage violations caused by excess power flow in feeders with significant impedance.

In this context, the specific contributions of this paper are: ① the definition of spatial and temporal indices to reveal the level and seriousness of congested area in radial distribution networks in terms of both thermal limit violations and voltage violations; ② the definition of indices of the relationships between the customers at each bus and each thermal/voltage congestion considering the average contribution, in order to identify both customers who are the leading cause of the congestion and those whose flexibilities may perform effectively in relieving congestions; ③ the suggestion on the use of the proposed indices for short-term CM procedures, flexibility market regulation, and long-term investment planning and expansion.

The paper is structured as follows. Section II presents quantitative indices for congestion levels. Section III describes indices of the relationship between users and congestions. Section IV presents the application of the method in the test cases considering daily profiles of load, PV generation, and EV charging requests. Section V describes the numerical tests relevant to the contributions of customers and the application to market-based CM schemes. Section VI concludes the paper.

II. QUANTITATIVE INDICES FOR CONGESTION LEVEL

The proposed quantitative indices for the evaluation of congestion levels are shown in Fig. 1, where $P+jQ$ is the bus load, e.g., P and Q are the active power load and reactive power load. Note that the dashed blue and red lines represent the signal transactions. Spatial indices indicate the violation of current and voltage limits at different branches and buses. Spatial indices for thermal violation include the maximum thermal violation M_{CI}, average thermal violation A_{CI}, and accumulative thermal violation A_{CCI}. Spatial indices for voltage violation include the maximum voltage violation M_{CV}, average voltage violation A_{CV}, and accumulative voltage violation A_{CCV}. Temporal indices reveal the seriousness of congestion in terms of frequency for thermal violation C_{RI} and voltage violation C_{RV}; and continuity for thermal violation C_{onici} and voltage violation C_{onicv}. Aggregate index of thermal violation A_{ICI} and voltage violation A_{ICV} are proposed to identify congested areas by combining spatial and temporal indices for thermal violation and voltage violation, respectively. For simplicity, all the described indices refer to a short-term horizon, typically a day. Long-term indices, e.g., for a month or a year, can be calculated by combining the clusters (typical days) with their probabilities.

Although we apply the proposed indices to three-phase networks under unbalanced conditions, the reference to a specific phase is avoided in the description for simplicity. If a phase conductor or the neutral of a branch is overloaded, we assume thermal congestion in that branch. The same applies for voltage violations at a bus, considering that both the maximum and minimum limits cannot be violated at the same bus and period for different phase voltages.
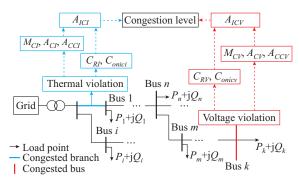
Fig. 1. Quantitative indices for evaluation of congestion levels.

A. Spatial Indices

Typical indices which are able to quantify spatial congestion levels are the maximum, average, and cumulative violation values both for branch currents and bus voltages in a specific period.

For a distribution network with N_{br} branches and N_{nd} buses, we define $\boldsymbol{B}$ as $N_{br} \times t_r$ matrix of branch current root mean square (RMS) values and $\boldsymbol{V}$ as the $N_{nd} \times t_r$ matrix of bus voltage RMS values at each interval Δt ($\sum \Delta t = t_r$, where t_r is the time horizon and equals to 24 hours in the simulations of Section IV, and Δt is the interval time, which is 1 hour for case 1 and 0.5 hour for case 2 in Section IV).

The relevant definitions at the tth interval are:

$$CI(i,t) = \begin{cases} \dfrac{\boldsymbol{B}(i,t) - \boldsymbol{I}_r(i)}{\boldsymbol{I}_r(i)} & \boldsymbol{B}(i,t) > \boldsymbol{I}_r(i) \\ \boldsymbol{0} & \boldsymbol{B}(i,t) \le \boldsymbol{I}_r(i) \end{cases} \quad (1)$$

$$CV(j,t) = \begin{cases} \left| \dfrac{\boldsymbol{V}(j,t) - V_{\max}}{V_N} \right| & V(j,t) > V_{\max} \\ \left| \dfrac{\boldsymbol{V}(j,t) - V_{\min}}{V_N} \right| & V(j,t) < V_{\min} \\ \boldsymbol{0} & V_{\min} \le V(j,t) \le V_{\max} \end{cases} \quad (2)$$

$$\boldsymbol{M}_{CI}(i) = \max\{\boldsymbol{CI}_{row^{(i)}}\} \quad (3)$$

$$\boldsymbol{A}_{CI}(i) = \dfrac{\sum\limits_{t=1}^{t_r} \boldsymbol{CI}(i,t)}{\boldsymbol{t}_c(i)} \quad (4)$$

$$\boldsymbol{A}_{CCI}(i) = \sum\limits_{t=1}^{t_r} \boldsymbol{CI}(i,t) \cdot \Delta t \quad (5)$$

where i, j, and t denote the branch, bus, and time, respectively; $\boldsymbol{CI}$ is the $N_{br} \times t_r$ matrix of thermal violations; $\boldsymbol{CV}$ is the $N_{nd} \times t_r$ matrix of voltage violations; $\boldsymbol{M}_{CI}$, $\boldsymbol{A}_{CI}$, and $\boldsymbol{A}_{CCI}$ are the maximum, average, and cumulative thermal violation $N_{br} \times 1$ vectors on all the branches, respectively; $\boldsymbol{M}_{CV}$, $\boldsymbol{A}_{CV}$, and $\boldsymbol{A}_{CCV}$ are the maximum, average, and cumulative voltage violation $N_{nd} \times 1$ vectors at all the buses, respectively; $\boldsymbol{I}_r$ is the $N_{br} \times 1$ vector of current rated values for all the branches; V_N is the rated voltage in per unit; $V_{\max}$ and $V_{\min}$ are the upper- and lower-voltage constraints, respectively, $V_{\max} = 1.05$ p.u., $V_{\min} = 0.95$ p.u.; and $\boldsymbol{t}_c$ is the $N_{br} \times 1$ vector of total thermal congestion durations in each branch.

$\boldsymbol{M}_{CV}$, $\boldsymbol{A}_{CV}$, and $\boldsymbol{A}_{CCV}$ are calculated with expression analogous to (3)-(5). For example, in the simulation on the IEEE 123-bus system shown in Section IV, A_{CCI}, A_{CI}, and M_{CI} of branch 1 are 4.487, 0.299, and 0.65, and the cumulative overloading is 4.487 p.u., whilst the average and the maximum overloadings are 0.299 and 0.65 p.u., respectively.

B. Temporal Indices

Temporal indices are proposed to quantify the congestion duration, frequency, and continuity. C_{RI} and C_{RV} are temporal indices that show the congestion duration in a specific time horizon. The vectors are defined as:

$$\boldsymbol{C}_{RI}(i) = \dfrac{\boldsymbol{t}_c(i)}{t_r} \times 100\% \quad (6)$$

$$\boldsymbol{C}_{RV}(i) = \dfrac{\boldsymbol{t}_v(i)}{t_r} \times 100\% \quad (7)$$

where $\boldsymbol{C}_{RI}$ is the $N_{br} \times 1$ vector of the ratio between the thermal violation durations in the branches and the time horizon; $\boldsymbol{C}_{RV}$ is the $N_{nd} \times 1$ vector of the ratio between voltage violation durations at the buses and the time horizon; and $\boldsymbol{t}_v$ is the $N_{nd} \times 1$ vector of the entire voltage congestion duration at each bus.

From the perspective of the CM procedure, congestions that last longer than a predefined time interval should have the priority. Some indices are specifically defined to reveal the degree of continuity of the congestion.

These values of these indices are obtained as described below. We define $\boldsymbol{S}_{ci}$ as the $N_{br} \times t_r$ matrix in which $\boldsymbol{S}_{ci}(i,t) = \text{sgn}(\boldsymbol{CI}(i,t))$ and $\boldsymbol{S}'_{ci}$ as the shifted matrix of $\boldsymbol{S}_{ci}$ by l time intervals:

$$\boldsymbol{S}'_{ci}(i,t) = \begin{cases} \boldsymbol{S}_{ci}(i,t-l) & l < t \le t_r \\ \boldsymbol{0} & 0 \le t \le l \end{cases} \quad (8)$$

Then, $\boldsymbol{C}_{onici}$ is given by:

$$\boldsymbol{C}_{onici}(i) = \dfrac{\boldsymbol{S}_{ci,row^{(i)}}(\boldsymbol{S}'_{ci,row^{(i)}})^{\text{T}}}{\boldsymbol{t}_c(i)} \times 100\% \quad (9)$$

where $\boldsymbol{C}_{onici}$ is the $N_{br} \times 1$ vector of thermal violation continuity indices; and $\boldsymbol{S}_{ci,row^{(i)}}$ is the ith row of $\boldsymbol{S}_{ci}$. The definition depends on the predefined value of l (equal to 1 for the simulations in Section IV). $\boldsymbol{C}_{onicv}$ is the $N_{nd} \times 1$ vector of voltage violation continuity indices, which is defined analogously and includes the definition of $\boldsymbol{S}_{cv}$ as the $N_{nd} \times t_r$ matrix with $\boldsymbol{S}_{cv}(j,t) = \text{sgn}(\boldsymbol{CV}(j,t))$, and $\boldsymbol{S}'_{cv}$ as the shifted matrix of $\boldsymbol{S}_{cv}$ by l time intervals. For example, in case 1 of Section IV, C_{RI} and C_{onici} of branch 1 are 62.5% and 73.33%, representing the overloading frequency per day and the continuity of overloading periods, respectively.

C. Aggregate Overload Index

A_{ICI} and A_{ICV} integrate the spatial and temporal indices in terms of thermal violation and voltage violation, respectively, for short- and long-term congestion estimations. These indices provide a clear vision of congestion scenarios and congested levels. The definitions are as follows.

$$\boldsymbol{A}_{ICI} = \boldsymbol{A}_{CI} \circ \boldsymbol{t}_c \circ \boldsymbol{C}_{onici} \quad (10)$$

$$\boldsymbol{A}_{ICV} = \boldsymbol{A}_{CV} \circ \boldsymbol{t}_v \circ \boldsymbol{C}_{onicv} \quad (11)$$

where ∘ denotes the element-by-element multiplication. For instance, in the simulations relevant to the Australian 23-bus system shown in Section IV, A_{ICI} and A_{ICV} of branch 10 and bus 23 at phase C are 2.4497 p.u. and 0.2024 p.u., respectively.

The calculation procedure of spatial and temporal indices is shown in Fig. 2. At first, the data of a typical day are selected. Then, the power flow calculation is performed. If there are congestions, all the indices relevant to both thermal congestion and voltage congestion are calculated according to the equations shown in the previous subsections.

Fig. 2.   Calculation procedure of spatial and temporal indices.

III. INDICES OF RELATIONSHIP BETWEEN USERS AND CONGESTIONS

For the case of thermal violations, in a radial distribution network, all the downstream buses of one congested branch/bus would contribute to the congestion of this branch/bus. For the case of voltage violations, the flexibility of customers connected upstream with respect to the affected area can be used by the CM procedure as they may be more effective than those in the other buses. After identifying the congestion level, the assessment of the specific relationship between each customer and congestion has significant importance in building a fairer market by allocating the duty for congestion alleviation. In this framework, specific indices are proposed to identify these relationships that can be exploited by electricity policy for rewarding proactive consumers to use local generation and DR mechanisms [30]-[33].

The proposed contribution of customer indices include the maximum, average, and standard deviations of contributions to thermal violations (max_{ci}, ave_{ci}, and std_{ci}) and voltage violations (max_{cv}, ave_{cv}, and std_{cv}), respectively. Aggregate contribution index A_{GCI} is also proposed to present the aggregate

contribution from one customer. The indices are illustrated in Fig. 3 and described in the following three subsections.
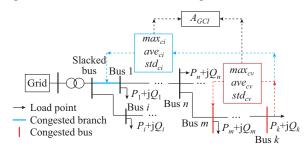

Fig. 3.   Overview of indices for contributions of customer.

Customers are aggregated at each bus due to two reasons. Firstly, in nodal price regulation, the knowledge of the aggregate contribution is more useful than the specific contribution from each single customer connected to the same bus. Secondly, the contribution from an individual customer can be calculated by multiplying the proportion of a single customer to the total. The load from a single customer is obtained by an appropriate metering infrastructure.

A. Contributions of Customer to Thermal Violation

To express the influence of bus currents on branch currents and voltage drops, the well-known matrices **BIBC** and **BCBV** are used. **BIBC** is the bus-injection to branch-current matrix, and **BCBV** is the branch-current to bus-voltage matrix [34].

We define the following spatial and temporal indices: CTV_k is the $N_{br} \times t_r$ matrix of the contributions of customer at bus k to the thermal violation during t_r; M_{ci} is the $N_{nd} \times t_r$ matrix of the number of congested branches influenced by the customers at each bus during t_r; t_{ci} is the $N_{nd} \times N_{br}$ matrix of the duration (in hour) of congestions in each branch due to the customers connected to each bus; and max_{ci}, ave_{ci}, and std_{ci} are the $N_{nd} \times 1$ vectors of maximum, average, and standard deviation values of the contributions from the customer at each bus to thermal violations, respectively.

We consider I as the $N_{nd} \times t_r$ matrix of the currents injected at the buses and CTV_k' as the $N_{br} \times t_r$ matrix of the ratios between the current in branch i due to the current injected at bus k and the total currents in the same branch:

$$CTV_k'(i,t) = \frac{BIBC(i,k) \cdot I(k,t)}{B(i,t)} \quad (12)$$

$$CTV_k(i,t) = \begin{cases} CTV_k'(i,t)\dfrac{B(i,t)-I_r(i)}{I_r(i)} & B(i,t)>I_r(i) \\ 0 & B(i,t) \leq I_r(i) \end{cases} \quad (13)$$

One customer may contribute to several congested branches. Also, the contributions from that customer varies according to the fluctuation of thermal violations. Therefore, the variation of contributions needs to be considered in evaluating the contribution in the short-term and long-term time horizon. We consider the max_{ci} and ave_{ci} are the mean values of the maximum and average contributions to all the congested branches throughout the thermal congested periods.

For instance, to calculate max_{ci} from the customer at bus k, the maximum contributions to all congested branches

from this customer are calculated separately at each interval firstly. Then, all the maximum contributions are added up and divided by the maximum congestion duration. The elements of $\boldsymbol{max}_{ci}$, $\boldsymbol{ave}_{ci}$, and $\boldsymbol{std}_{ci}$ are calculated as:

$$\boldsymbol{max}_{ci}(k)= \sum_{t=1}^{t_r}\max\{\boldsymbol{CTV}_{k,column^{(t)}}\}\Big/\max\{\boldsymbol{t}_{ci,row^{(k)}}\} \qquad (14)$$

$$\boldsymbol{ave}_{ci}(k)= \sum_{t=1}^{t_r}\frac{\sum \boldsymbol{CTV}_k(i,t)}{\boldsymbol{M}_{ci}(k,t)}\Big/\max\{\boldsymbol{t}_{ci,row^{(k)}}\} \qquad (15)$$

$$\boldsymbol{std}_{ci}(k)= \frac{\sum_{t=1}^{t_r}\dfrac{\sqrt{\sum_i\left(\boldsymbol{CTV}_k(i,t)-\overline{\boldsymbol{CTV}}_{k,row^{(i)}}\right)^2}}{\boldsymbol{M}_{ci}(k,t)}}{\max\{\boldsymbol{t}_{ci,row^{(k)}}\}} \qquad (16)$$

where $\overline{\boldsymbol{CTV}}_{k,row^{(i)}}$ is the mean of the elements of row i of matrix $\boldsymbol{CTV}_k$. For example, in case 1 of the simulations in Section V, the maximum and average contributions from customers at bus 48 with configuration 1 to overloading are 0.0495 p.u. and 0.0431 p.u., respectively.

B. Contributions of Customers to Voltage Violation

Analogously to the relationship between customers and the thermal violations in the branches, we define the following indices for the contributions to the bus voltage violations: $\boldsymbol{CVV}_k$ is the $N_{nd}\times t_r$ matrix of the contributions of customers at bus k to voltage violation during t_r; $\boldsymbol{M}_{cv}$ is the $N_{nd}\times t_r$ matrix of the number of congested buses caused by each bus current during t_r; $\boldsymbol{t}_{cv}$ is the $N_{nd}\times N_{nd}$ matrix of the duration of the congestion on each bus caused by each bus current; and $\boldsymbol{max}_{cv}$, $\boldsymbol{ave}_{cv}$, and $\boldsymbol{std}_{cv}$ are the $N_{nd}\times 1$ vectors of the maximum, average, and standard deviation values of the contributions of each bus current to voltage violations, respectively.

For the calculation of $\boldsymbol{CVV}_k$, we define at first $\boldsymbol{CVV}'_k$ as the $N_{nd}\times t_r$ matrix of the ratios between the voltage drop due to the current at bus k and the total voltage drop at the same bus as:

$$\boldsymbol{CVV}'_k(j,t)= \frac{\boldsymbol{DLF}(j,k)\boldsymbol{I}(k,t)}{\Delta\boldsymbol{V}(j,t)} \qquad (17)$$

where $\boldsymbol{DLF}=\boldsymbol{BCBV}\cdot\boldsymbol{BIBC}$. Then, we can obtain:

$$\boldsymbol{CVV}_k(j,t)= \begin{cases} \boldsymbol{CVV}'_k(j,t)(\boldsymbol{V}(j,t)-V_{max}/V_N) & V(j,t)>V_{max} \\ \boldsymbol{CVV}'_k(j,t)(\boldsymbol{V}(j,t)-V_{min}/V_N) & V(j,t)<V_{min} \\ 0 & \text{otherwise} \end{cases} \qquad (18)$$

C. Contribution of Customer at Each Bus to Congested Area

$\boldsymbol{A}_{GCI}$ shows the contribution of the customer at each bus to the congested areas, considering both thermal and voltage violations. For its calculation, at first, the total contribution of the injected current at bus k to the congested branches and buses is evaluated for each time slot. Then, the two contributions are weighted by using the vectors of coefficients $\boldsymbol{C}_1$ and $\boldsymbol{C}_2$. Finally, $\boldsymbol{A}_{GCI}(k)$ is calculated as the contribution over the total duration of congestions:

$$\boldsymbol{A}_{GCI}(k)= \frac{\sum_{t=1}^{t_r}\left(\boldsymbol{C}_1(t)\sum\boldsymbol{CTV}_k(i,t)+\boldsymbol{C}_2(t)\sum\boldsymbol{CVV}_k(i,t)\right)}{N(k)} \qquad (19)$$

$\boldsymbol{C}_1$ and $\boldsymbol{C}_2$ allow for weighting the contributions to thermal congestion and voltage congestion, respectively, which can be decided by the customer damage function (CDF) or value of customer reliability (VCR). Since CDF or VCR is not in the scope of this paper, $\boldsymbol{C}_1$ and $\boldsymbol{C}_2$ are considered equal to 0.5. $N(k)$ is the total duration of congestions due to the injected current at bus k, i.e., $N(k)=\max\{\boldsymbol{t}_{ci,row^{(k)}},\boldsymbol{t}_{cv,row^{(k)}}\}$.

IV. ILLUSTRATIVE RESULTS OF PROPOSED INDICES

Two test cases are considered: case 1 uses the IEEE 123-bus test system [35] considering two different configurations. In case 1, we assume a 100% penetration of EV and 40% penetration of PV generation, i.e., the ratio between the total EV or PV capacity and the peak load. Case 2 uses the Australian 23-bus low-voltage (LV) distribution network [36] considering 30% penetration of EV.

Regarding case 1, Fig. 4 shows the active power P and reactive power Q of spot load at each bus. The load at each interval is obtained by combining rated power and the daily load demand profile (p.u.) from [29]. For simplicity, each node has the same daily profile. Analogously, Fig. 5 shows the maximum active and reactive power of case 2, considering the presence of PV generation. We have assumed the interval time $\Delta t=1$ hour for case 1 and $\Delta t=0.5$ hour for case 2, respectively.
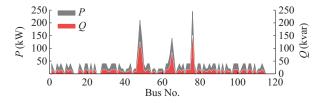

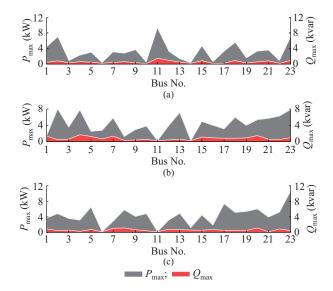Fig. 4.   Spot load at each bus of case 1.

Fig. 5.   Maximum active and reactive power of case 2. (a) Phase A. (b) Phase B. (c) Phase C.

In both cases, the load demand of EV charging has been obtained by using the profiles of weighted arrival time probability distribution from [37] and state-of-charge (SoC) difference from [38] due to the charging process. Although it is

an effective method of relieving congestions, smart charging is not considered in this paper.

We assume a constant that voltage equals to the rated value at the medium-voltage (MV) side of the substation transformer due to the action of its automatic voltage regulator. I_r for branches 1 (between buses 149 and 1), 4, 8, 11, 14, 37, 42, 44, 46, 49-54, 56, 59, 115 (between buses 18 and 35), 117 (between buses 13 and 52), and 119 (between buses 54 and 94) is 200 A; I_r for branches 73, 78, 87, 89, 91, 93, 94, 102, 106, 109, 119 (between buses 97 and 197), 121 (between buses 151 and 300) is 150 A; and I_r for the rest of branches is 100 A in case 1. I_r of branches 7, 9, 10, 15, 16, 17 is 200 A, and 100 A for the rest of the branches in case 2. Also, each branch is named by the number of receiving bus in case 2.

A. Case 1

As mentioned above, two different configurations of the IEEE 123-bus test distribution feeder are considered. In configuration 1, switches 1, 2, 3, 6, and 7 are closed, while switches 4 and 5 are open. The voltage regulator between bus 160 and bus 67 is operating within a 10% maximum range. In configuration 2, switches 1, 2, 3, 4, and 5 are closed, and switches 6 and 7 are open. The voltage regulator between bus 25 and bus 26 is in operation.

Figures 6 and 7 show the simulation results of the proposed spatial and temporal indices of congested branches and buses for configuration 1, respectively. Branches 1, 4, 8, 11, 53, and 116 are congested due to thermal violations. Among those congested branches, branch 1 experiences the most severe thermal violation. A_{CCI}, A_{CI}, and M_{CI} of branch 1 are 4.487, 0.299, and 0.65, respectively. Concerning congestion duration, 62.5% of a day is congested with the continuity index equal to 73%. Buses from 44 to 51 are congested due to voltage violations for one hour, with similar A_{CCV}, A_{CV}, and M_{CV}, which are around 0.001-0.004.
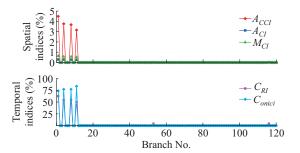

Fig. 6.   Spatial and temporal indices of congested branches for configuration 1.
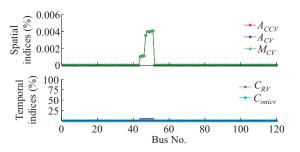

Fig. 7.   Spatial and temporal indices of congested buses for configuration 1.

Figures 8 and 9 show the simulation results of spatial and temporal indices of congested branches and buses for configuration 2. As in configuration 1, branches 1, 4, 8, 11, 38, 95, 96, and 119 are suffering from thermal violation, but a larger number of buses are congested. Moreover, the congestion levels are higher than those in configuration 1 around 0.0013-0.034.
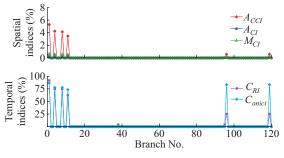

Fig. 8.   Spatial and temporal indices of congested branches for configuration 2.
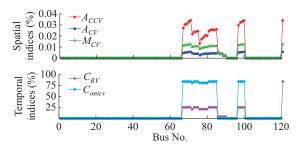

Fig. 9.   Spatial and temporal indices of congested buses for configuration 2.

Figure 10 shows the congestion map based on A_{ICI} and A_{ICV} values of configurations 1 and 2. Compared with configuration 1, the thermal congestion level of the second configuration is slightly lower with more congested branches. However, the increased number of congested buses shows that the chance of configuration has a substantial impact on voltage values in this case.

It is worth noting that the congested buses of configuration 1 experience voltage violations for 1 hour. According to the definition ($l = 1$ hour for case 1), A_{ICV} values of congested buses in configuration 1 are equal to 0, implying that the voltage issue can be ignored in this scenario. As for configuration 2, even though the A_{ICV} values of buses 67-85 and 97-100 are not as high as A_{ICI}, voltage violation cannot be neglected by power utilities. Furthermore, the priority in the application of CM procedure should be considered according to the VCR.

B. Case 2

According to Fig. 11, branches 7, 9, and 10 at phase A are suffering from thermal violations. Branches 1, 2, 7, 9, 10, 15, 16, and 21 at phases B and C experience thermal violations. The maximum A_{CI} values of congested branches at phases A, B, and C are 0.29 p.u., 0.43 p.u., and 0.53 p.u., respectively. Branches 7, 9, and 10 experience the most severe thermal violation since each phase is congested.
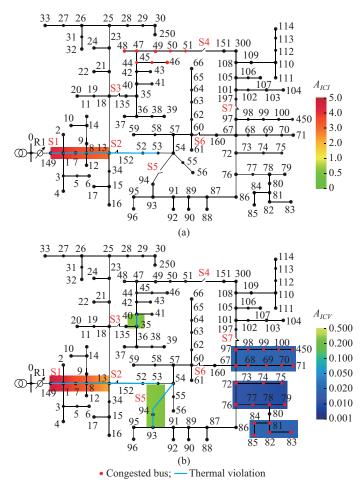
Fig. 10.   Congestion map based on A_{ICI} and A_{ICV}. (a) A_{ICI} of configuration 1. (b) A_{ICI} and A_{ICV} of configuration 2.
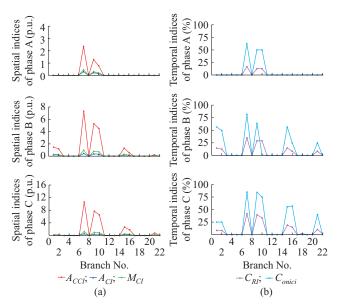

Fig. 11.   Spatial and temporal indices of congested branches at each phase of case 2. (a) Spatial indice. (b) Temporal indice.

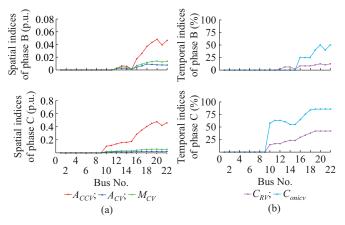Fig. 12.   Spatial and temporal indices of congested buses at each phase of case 2. (a) Spatial indice. (b) Temporal indice.

Phases B and C suffer longer congestion, over 30% of the time horizon. In summary, phase C experiences the severest thermal violation compared with the other two phases. Also, no voltage congestion occurs in phase A.

Figure 12 illustrates the spatial and temporal indices of congested buses at each phase of case 2. 41.67% of the time horizon at phase C and 12.5% of the time horizon at phase B suffer from voltage violations.

The maximum continuities of voltage congestion at phases B and C are 20 % and 83.33%, respectively. More buses with higher voltage violations encounter voltage violations at phase C. Overall, phase C is more vulnerable than the other

two phases in terms of thermal violation and voltage violation.

The Australian 23-bus LV distribution feeder, shown in Fig. 13, is characterized by unbalanced loads. Figure 13 also shows thermal congestion map at each phase based on A_{ICI} of case 2.
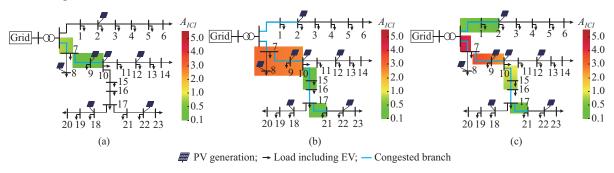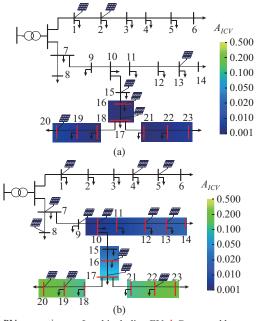

Fig. 13.   Thermal congestion map at each phase based on A_{ICI} of case 2. (a) Phase A. (b) Phase B. (c) Phase C.

According to these maps, phase C suffers the most serious congestions compared with phases A and B in terms of both thermal and voltage violations. Figure 14 shows voltage congestion map at phases B and C based on A_{ICV} of case 2. Phase C suffers the most serious congestion in terms of the number of congested buses and A_{ICV}. In summary, phase C experiences the most serious congestion issue among the three phases, in terms of magnitude violation and duration.

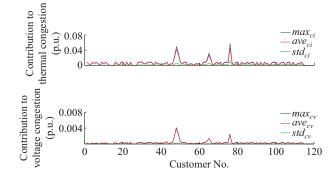Fig. 14. Voltage congestion map at phases B and C based on A_{ICV} of case 2. (a) Phase B. (b) Phase C.

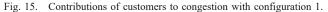## V. ILLUSTRATIVE RESULTS OF CONTRIBUTIONS OF CUSTOMER INDICES

A. Case 1

Contributions of customers to congestion with configuration 1 is presented in Fig. 15. The customer at bus 48 contributes the most to the thermal violation in branches and the voltage violation at buses. Figure 16 shows the contributions of customers to congestion with configuration 2. The most significant contribution is from the customer at bus 76, followed by the customer at bus 48. The customer at bus 48 contributes slightly more than the customer at bus 65. Figure 17 shows A_{GCI} of load at each bus for the two configurations. Considering the numbers of congested branches and buses influenced, the values of A_{GCI} at buses 76, 48, and 67 are larger than other buses, showing that the average contributions from the customers at those buses to thermal and voltage violations are higher than other customers. Also, it suggests that regulating load consumption from those buses will be more effective in CM.

B. Case 2

For Case 2, the average and maximum contributions of customers to thermal violations and voltage violations at three phases are shown in Fig. 18.

Fig. 15. Contributions of customers to congestion with configuration 1.
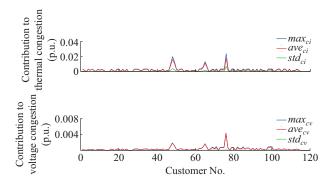

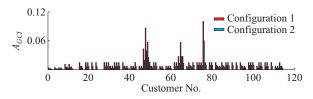Fig. 16. Contributions of customers to congestion with configuration 2.

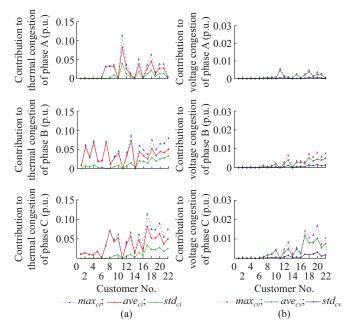Fig. 17. A_{GCI} of load at each bus.

Fig. 18. Contribution of customer to congestion at each bus for case 2. (a) Contribution to thermal congestion. (b) Contribution to voltage congestion.

Customers at bus 11, followed by customers at bus 23, contribute the most to the congestion in phase A. Customers at buses 2, 4, 7, 13, 18, 22, and 23 contribute more than 0.05 p.u. to the thermal violation in phase B. Customers at buses 17 and 23 contribute more than 0.08 p.u. to the thermal violation in phase C. Similarly, customers, with the largest contributions to the thermals violation, also contribute the most to voltage violation in phases B and C.

Figure 19 presents the A_{GCI} of customers at each phase. Customers at phase C contribute the most to the congestion compared with the customers connected at phases B and A. Customers at buses from 1 to 6 have the minimum contributions to congestions since there is no voltage violation with a trivial thermal violation at the corresponding branches and buses. In total, the customer at bus 23 contributes the most to the congestion in the network, considering the numbers of congested branches and buses.
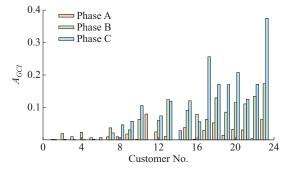

Fig. 19. A_{GCI} of customers at each bus for case 2.

As expected, the buses with higher injected currents show significant contributions to congestions. Customers connected to the buses at the end of the feeder exhibit larger contributions than those connected with buses near the substation, even though they have similar loads. Moreover, different configurations may lead to different contributions, even though the loads are not changed. The number of congested branches and buses is another critical factor that influences the aggregative contribution index.

C. Application of Proposed Indices by Utility Operators

In the simulation, the time horizon is 24 hours (a day) with intervals of 1 hour and 0.5 hour for case 1 and case 2. Long-term, e.g., one year or five years, congestion estimation can be attained by clustering the load with probabilities and application of the same procedures as presented in this paper. The evaluation of the proposed indices for congestion areas and contributions of customer can help power utility to regulate proper CM procedures and build a fair market for the active customers, especially when the flexibilities are limited as well as make long-term investment plans.

For a short-term congestion estimation, e.g., 24 hours, vulnerable areas can be detected by calculating the proposed indices for thermal and voltage violations based on the load forecasting for the next following 24 hours. The most vulnerable regions for thermal congestion and voltage congestion can be distinguished by checking the congestion severity map according to the A_{ICI} and A_{ICV} values. Spatial and tempo-

ral indices provide detailed information on congested branches and buses in these vulnerable areas. With the thermal vulnerable area map and voltage vulnerable map, power utilities can prioritize the areas according to the seriousness of congestion and regulate short-term CM procedures.

Moreover, evaluating the proposed indices for contributions of customer to congestions helps build fairer flexibility management and regulation of rewards for the customers contributing to congestion solution. According to [39], the capability to discover the location where flexibility is needed is a necessity for an active distribution market. The proposed contribution of customer indices can help power utilities to recognize the areas in which responses from active customers to CM procedures have a better outcome than other areas. Following the scheme of electricity market proposed in [40], the customers triggering the volatility need to be appropriately penalized. However, the reward policy that encourages customers to participate in the CM is also important. For improving customer participation, customers can be classified into different clusters based on the values of contribution indices. Furthermore, the proposed indices both for quantifying the seriousness of congestion and contributions of customer can also be utilized for the evaluation of the effectiveness of specific CM strategies and adjustment of real-time spot price during the congestion.

Investment planning referencing the long-term congestion estimation can help power utilities to relieve the congestion and improve system reliability. For instance, the deployment of energy storage system (ESS) can shave load and absorb excessive renewable generation in a distribution network integrated with high penetration of DER [39]. Also, ESS is a suitable option for the long-term management of congestion. The drawback of the utilization of ESS is its high cost. Long-term estimation of congested areas is vital in determining an appropriate budget by finding the lowest cost and optimal location of ESS. As proposed in this paper, the correct understanding of the CM indices enhances the procedure of decision-making in long-term planning. Moreover, encouraging the investment from customers in the areas in which congestion happens frequently and customers have better performance over others in response to CM procedures can reduce power loss and implement flexibilities in distribution networks. The application of the proposed indices is shown in Fig. 20.
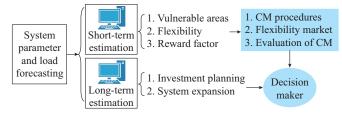

Fig. 20.   Application of proposed indices.

VI. Conclusion

In this paper, we propose spatial indices and temporal indices to quantify the seriousness of congestions in distribution network in terms of both thermal violation and voltage viola-

tions. Spatial indices include the maximum, average, and cumulative values of thermal and voltage magnitude violations. Temporal indices are congestion duration, congestion rate, and continuity. Two aggregate congestion level indices are proposed to represent the congestion level of thermal and voltage violations considering the frequencies and continuities in the long term. Also, the contribution indices from customers to thermal congestion and voltage congestion are represented in this paper as well as the aggregate index.

Numerical results obtained using the IEEE 123-bus test feeder with two configurations and an Australian 23-bus LV distribution system confirm that the proposed indices can be utilized to quantify the seriousness of congestions from perspectives of amplitude violation and duration in a balanced system and an unbalanced system.

For the considered cases, changing the system configuration has more impacts on voltage congestion compared with thermal congestion. The congestion may exacerbate the voltage unbalance issue. The proposed indices can identify the severity of the congestions, the geographical location of concerned areas, and contributions of customer. Moreover, suggestions on the deployment of the proposed indices for applying demand response or regulating electricity price in CM procedure are presented.

Concerning traditional indices that only consider the magnitude of violation at a specific load point, the aggregated indices that consider the duration and spatial will help make better decisions relevant to CM policy and strategies in the situations of limited flexibility resources.

REFERENCES

[1] S. Bahramirad, A. Khodaei, and R. Masiello, "Distribution markets," *IEEE Power & Energy Magazine*, vol. 14, no. 2, pp. 102-106, Apr. 2016.

[2] M. Mao, S. Zhang, L. Chang *et al.*, "Schedulable capacity forecasting for electric vehicles based on big data analysis," *Journal of Modern Power Systems and Clean Energy*, vol. 7, no. 6, pp. 1651-1662, Nov. 2019.

[3] A. Samimi, "Probabilistic day-ahead simultaneous active/reactive power management in active distribution systems," *Journal of Modern Power Systems and Clean Energy*, vol. 7, no. 6, pp. 1596-1607, Nov. 2019.

[4] F. R. Badal, P. Das, S. K. Sarker *et al.*, "A survey on control issues in renewable energy integration and mircrogrid," *Protection and Control of Modern Power Systems*, vol. 4, no. 8, pp. 87-113, Dec. 2019.

[5] N. I. Yusoff, A. A. M. Zin, and A. B. Khairuddin, "Congestion management in power system: a review," in *Proceedings of 3rd International Conference on Power Systems and Renewable Energy Technologies (PGSRET)*, Johor Bahru, Malaysia, Apr. 2017, pp. 22-27.

[6] J. Zhao, A. Arefi, A. Borghetti *et al.*, "Characterization of congestion in distribution network considering high penetration of PV generation and EVs," in *Proceedings of IEEE PES General Meeting*, Atlanta, USA, Aug. 2019, pp. 1-5.

[7] S. Huang, Q. Wu, Z. Liu *et al.*, "Review of congestion management methods for distribution networks with high penetration of distributed energy resources," in *Proceedings of IEEE PES Innovative Smart Grid Technologies*, Istanbul, Turkey, Oct. 2014, pp. 1-6.

[8] H. Sagha, G. Mokhtari, A. Arefi *et al.*, "A new approach to improve PV power injection in LV electrical systems using DVR," *IEEE Systems Journal*, vol. 12, no. 4, pp. 3324-3333, Dec. 2018.

[9] H. Pezeshki, A. Arefi, G. Ledwich *et al.*, "Probabilistic voltage management using OLTC and D-STATCOM in distribution networks," *IEEE Transactions on Power Delivery*, vol. 33, no. 2, pp. 570-580, Apr. 2018.

[10] K. Geschermann and A. Moser, "Evaluation of market-based flexibility provision for congestion management in distribution grids," in *Pro-*
ceedings of IEEE PES General Meeting, Chicago, USA, Jul. 2017, pp. 1-5.

[11] A. Borghetti, M. Bosetti, S. Grillo *et al.*, "Short-term scheduling and control of active distribution systems with high penetration of renewable resources," *IEEE System Journal*, vol. 4, no. 3, pp. 313-322, Sept. 2010.

[12] B. Kirby and J. V. Dyke, *Congestion Management Requirements, Methods and Performance Indices*. Oak Ridge: Oak Ridge National Laboratory, Jun. 2002.

[13] Q. Zhou, L. Tesfatsion, and C. Liu, "Short-term congestion forecasting in wholesale power markets," *IEEE Transactions on Power Systems*, vol. 26, no. 4, pp. 2185-2196, Nov. 2011.

[14] E. Jonckheere, R. Banirazi, and E. Grippo, "Congestion management for cost-effective power grid load balancing using FACTS and energy storage devices allocated via grid curvature means," in *Proceedings of 2019 American Control Conference (ACC)*, Philadelphia, USA, Jul. 2019, pp. 3909-3915.

[15] F. Zaeim-Kohan, H. Razmi, and H. Doagou-Mojarrad, "Multi-objective transmission congestion management considering demand response and generation rescheduling," *Applied Soft Computing*, vol. 70, pp. 169-181, Jan. 2018.

[16] Y. T. Yoon, S. G. Raikar, and M. D. Ilic, *Congestion Management for Large Electric Power Systems*. Cambridge: Energy Laboratory Publication, 2000.

[17] M. Khanabadi, Y. Fu, and C. Liu, "Decentralized transmission line switching for congestion management of interconnected power systems," *IEEE Transactions on Power Systems*, vol. 33, no. 6, pp. 5902 - 5912, May 2018.

[18] S. A. Hosseini, N. Amjady, M. Shafie-khah *et al.*, "A new multi-objective solution approach to solve transmission congestion management problem of energy markets," *Applied Energy*, vol. 165, pp. 462-471, Mar. 2016.

[19] D. T. Phan and S. Ghosh, "Predicting and mitigating congestion for an electric power system under load and renewable uncertainty," in *Proceedings of 2016 American Control Conference (ACC)*, Boston, USA, Jul. 2016, pp. 6791-6796.

[20] S. Huang, Q. Wu, M. Shahidehpour *et al.*, "Dynamic power tariff for congestion management in distribution networks," *IEEE Transactions on Smart Grid*, vol. 10, no. 2, pp. 2148-2157, Mar. 2019.

[21] S. Huang and Q. Wu, "Dynamic tariff-subsidy method for PV and V2G congestion management in distribution networks," *IEEE Transactions on Smart Grid*, vol. 10, no. 5, pp. 5851-5860, Sept. 2019.

[22] A. Hermann, J. Kazempour, S. Huang *et al.*, "Congestion management in distribution networks with asymmetric block offers," *IEEE Transactions on Power Systems*, vol. 36, no. 4, pp. 4382-4392, Apr. 2019.

[23] J. Verboomen, G. Papaefthymiou, W. L. Kling *et al.*, "Use of phase shifting transformers for minimizing congestion risk," in *Proceedings of the 10th International Conference on Probabilistic Methods Applied to Power Systems*, Rincon, USA, May 2008, pp. 1-6.

[24] P. Chen, Z. Chen, and B. Bak-Jensen, "Probabilistic load flow: a review," in *Proceedings of Third International Conference on Electric Utility Deregulation and Restructuring and Power Technologies*, Nanjing, China, Apr. 2008, pp. 1586-1591.

[25] T. Ghose, H. W. Pandey, and K. R. Gadham, "Risk assessment of microgrid aggregators considering demand response and uncertain renewable energy sources," *Journal of Modern Power Systems and Clean Energy*, vol. 7, no. 6, pp. 1619-1631, Nov. 2019.

[26] H. Liao and J. V. Milanovic, "Flexibility exchange strategy to facilitate congestion and voltage profile management in power networks," *IEEE Transactions on Smart Grid*, vol. 10, no. 5, pp.4786-4794, Sept. 2018.

[27] A. N. M. M. Haque, P. H. Nguyen, F. W. Bliek *et al.*, "Demand response for real-time congestion management incorporating dynamic thermal overloading cost," *Sustainable Energy, Grids and Networks*, vol. 10, pp. 65-74, Jan. 2017.

[28] S. Gope, A. K. Goswami, P. K. Tiwari *et al.*, "Rescheduling of real power for congestion management with integration of pumped storage hydro unit using firefly algorithm," *Electrical Power and Energy Systems*, vol. 83, pp. 434-442, Dec. 2016.

[29] A. Narimani, G. Nourbakhsh, A. Arefi *et al.*, "SAIDI constrained economic planning and utilization of central storage in rural distribution networks," *IEEE Systems Journal*, vol. 13, pp. 842-853, Mar. 2019.

[30] H. Emami and J. A. Sadri, "Congestion management of transmission lines in the market environment," *International Research Journal of Applied and Basic Sciences*, vol. 3, pp. 2572-2580, Mar. 2012.

[31] S. W. Alnaser and L. F. Ochoa, "Hybrid controller of energy storage and renewable DG for congestion management," in *Proceedings of*

IEEE PES General Meeting, San Diego, USA, Jul. 2012, pp. 1-8.

[32] E. Amicarelli, T. Q. Tran, and S. Bacha, "Flexibility service market for active congestion management of distribution networks using flexible energy resources of micro-grids," in *Proceedings of IEEE PES Innovative Smart Grid Technologies Conference Europe (ISGT-Europe)*, Torino, Italy, Sept. 2017, pp. 1-6.

[33] A. Yousefi, T. T. Nguyen, H. Zareipour *et al.*, "Congestion management using demand response and FACTS devices," *Electrical Power and Energy Systems*, vol. 37, pp. 78-85, May 2012.

[34] J. H. Teng. "A direct approach for distribution system load flow solutions," *IEEE Transactions on Power Delivery*, vol. 18, no. 3, pp. 882-887, Jul. 2003.

[35] IEEE PES AMPS DSAS Test Feeder Working Group. (2015, Jan.). [Online]. Available: http://sites. ieee. org/pes-testfeeders/resources/123-bus Feeder.

[36] A. Forbes. (2018, Jan.). Customer-side voltage regulation to mitigate PV-induced power quality problems in radial distribution networks. [Online]. Available: https://www. semanticscholar. org/paper/Customer-Side-Voltage-Regulation-to-Mitigate-Power-Forbes/f39dcd5a99c7f59436af59ffb6003bf2a9c955fb.

[37] D. Fischer, A. Harbrech, A. Surmann *et al.*, "Electrical vehicles' impacts on residential electric local profiles – a stochastic modelling approach considering socio-economic, behavioral and spatial factors," *Applied Energy*, vol. 233, pp. 644-658, Feb. 2019.

[38] P. K. Dost, P. Spichartz, and C. Sourkounis, "Charging behavior of users utilizing battery electric vehicles and extended range electric vehicles within the scope of a field test," *IEEE Transactions on Industrial Application*, vol. 54, no. 1, pp. 580-590, Jan. 2018.

[39] A. Akrami, M. Doostizadeh, and F. Aminifar, "Power system flexibility: an overview of emergence to evolution," *Journal of Modern Power Systems and Clean Energy*, vol. 7, no. 5, pp. 987-1007, Sept. 2019.

[40] G. Tsaousoglou, P. Makris, and E. Varvarigos, "Electricity market policies for penalizing volatility and scheduling strategies: the value of aggregation, flexibility, and correlation," *Sustainable Energy, Grids and Networks*, vol. 12, pp. 57-68, Nov. 2017.

Jinping Zhao received the B.S. degree and M.S. degree in electrical engineering and automation from Lanzhou University of Technology, Lanzhou, China, in 2007 and 2011, respectively. Currently, she is a Ph.D. student at Murdoch University, Perth, Australia. Her research interests include power system planning, congestion management, and power quality.

Ali Arefi received the B.Sc. (honors), M.Sc., and Ph.D. degrees in electrical engineering in 1999, 2001, and 2011, respectively. He has been a Lecturer and Research Fellow in Queensland University of Technology (QUT), Brisbane, Australia, since 2012. Currently, he is a Senior Lecturer in Murdoch University, Perth, Australia. His research interests include sustainable and resilient planning of power delivery system, microgrid, smart grid, state estimation and so on.

Alberto Borghetti graduated in electrical engineering from the University of Bologna, Bologna, Italy, in 1992. Since then he has been working with the power system group of the same university, where he is now a Professor of electrical power systems. He is the IEEE Fellow (class 2015). Currently he is serving as an Editor of IEEE Transactions on Power Systems, as an Associate Editor of MPCE, and as Editor-in-Chief of Electrical Engineering-Archiv fur Elektrotechnik. His research interests include power system analysis, electromagnetic transients, optimal generation scheduling, and distribution system operation.

Gerard Ledwich received the Ph.D. degree in electrical engineering from the University of Newcastle, Newcastle, Australia, in 1976. Since 1998, he has been the Chair Professor in Electrical Power Engineering with Queensland University of Technology, Brisbane, Australia. From 1997 to 1998, he was the Head of the Department of Electrical Engineering, University of Newcastle, Newcastle, Australia. From 1976 to 1994, he was with the University of Queensland, Brisbane, Australia. He is a Fellow of the Institute of Engineers, Australia, and of the Institute of Electrical and Electronics Engineers. His research interests include power systems, power electronics, and wide area control of smart grids.